

FiLM: Frequency improved Legendre Memory Model for Long-term Time Series Forecasting

Abstract

Recent studies have shown the promising performance of deep learning models (e.g., RNN and Transformer) for long-term time series forecasting. These studies mostly focus on designing deep models to effectively combine historical information for long-term forecasting. However, the question of how to effectively represent historical information for long-term forecasting has not received enough attention, limiting our capacity to exploit powerful deep learning models. The main challenge in time series representation is how to handle the dilemma between accurately preserving historical information and reducing the impact of noisy signals in the past. To this end, we design a **Frequency improved Legendre Memory** model, or **FiLM** for short: it introduces Legendre Polynomial projections to preserve historical information accurately and Fourier projections plus low-rank approximation to remove noisy signals. Our empirical studies show that the proposed FiLM improves the accuracy of state-of-the-art models by a significant margin (**19.2%, 22.6%**) in multivariate and univariate long-term forecasting, respectively. In addition, dimensionality reduction introduced by low-rank approximation leads to a dramatic improvement in computational efficiency. We also demonstrate that the representation module developed in this work can be used as a general plug-in to improve the performance of most deep learning modules for long-term forecasting.

1 Introduction

Long-term time series forecasting has been a long-standing challenge in numerous applications (e.g., energy, weather, traffic, economics). Non-deep learning methods (e.g., ARIMA) often yield poor prediction results, due to the challenges of non-stationary time series, nonlinear dynamics, and complex patterns – common issues for long-term forecasting. Despite the early success of RNN-type deep learning methods for time series forecasting [Rangapuram et al. \(2018\)](#); [Salinas et al. \(2020\)](#), they often suffer from the problem of gradient vanishing/exploding [Pascanu et al. \(2013\)](#), significantly limiting their performance. Following the recent success in NLP and CV community [Vaswani et al. \(2017\)](#); [Devlin et al. \(2019\)](#); [Dosovitskiy et al. \(2021\)](#); [Rao et al. \(2021\)](#), Transformer [Vaswani et al. \(2017\)](#) has been introduced to capture long-term dependencies in time series forecasting and shows promising results [Zhou et al. \(2021\)](#); [Wu et al. \(2021\)](#); [Zhou et al. \(2022\)](#); [Wen et al. \(2022\)](#). A through overview of this line of work (Including deep recurrent networks and efficient Transformers) can be found in [Appendix A](#).

Most deep learning researchers focused on increasing model complexity by combining historical information better for accurate and reliable prediction. However, these methods may not capture all the critical historical signals and patterns for future forecasting with solely focusing on learning the combination. It is demonstrated in [Figure 1](#), where we compare the time series of ground truth with those predicted by the vanilla Transformer method and LSTM model [Vaswani et al. \(2017\)](#); [Hochreiter & Schmidhuber \(1997a\)](#) on a real-world ETTm1 dataset [Zhou et al. \(2021\)](#). It is observed that the predicted time series shared a *different* distribution from the ground truth. So historical

recovery and robustness for error propagation are two critical problems for long-term time series forecasting since we assume most forecasted sequences should maintain some historical statistics robustly. As a result, a good forecasting model should provide appropriate data representations that capture the important patterns in the past without being derailed by noisy signals.

This observation motivates us to switch our view from long-term time series forecasting to long-term sequence compression. Recursive memory model [Voelker et al. \(2019\)](#); [Gu et al. \(2021a,b, 2020\)](#) has achieved impressive results in function approximation tasks. [Voelker et al. \(2019\)](#)

designed a recursive memory unit (LMU) using Legendre projection, which provides a good representation for long time series. S4 model [Gu et al. \(2021a\)](#) comes up with another recursive memory design for data representation and significantly improves state-of-the-art results for Long-range forecasting benchmark (LRA) [Tay et al. \(2020b\)](#). However, when coming to long-term time series forecasting, these approaches fall short of the Transformer-based methods' state-of-the-art performance. A careful examination reveals that these data compression methods are powerful in recovering the details of historical data compared to LSTM/Transformer models, as revealed in Figure 2. However, they are vulnerable to noisy signals as they tend to overfit all the spikes in the past, leading to limited long-term forecasting performance. It is worth noting that, Legendre Polynomial employed in LMP [Voelker et al. \(2019\)](#) is just a special case in the family of Orthogonal Polynomials (OPs). OPs (including Legendre, Laguerre, Chebyshev, etc.) and other orthogonal basis (Fourier and Multiwavelets) are widely studied in numerous fields and recently brought in deep learning [Wang et al. \(2018\)](#); [Gupta et al. \(2021\)](#); [Zhou et al. \(2022\)](#); [Voelker et al. \(2019\)](#); [Gu et al. \(2020\)](#). A detailed review can be found in Appendix A.

The above observation inspires us to develop methods for accurate and robust representations of time series data for future forecasting, especially long-term forecasting. The proposed method significantly outperforms existing long-term forecasting methods on multiple benchmark datasets by integrating those representations with powerful prediction models. As the first step towards this goal, we directly exploit the Legendre projection, which is used by LMU [Voelker et al. \(2019\)](#) to update the representation of time series with fixed-size vectors dynamically. This projection layer will then be combined with different deep learning modules to boost forecasting performance. The main challenge with directly using this representation is the dilemma between information preservation and data overfitting, i.e., the larger the number of Legendre projections is, the more the historical data is preserved, but the more likely noisy data will be overfitted. Hence, as a second step, to reduce the impact of noisy signals on the Legendre projection, we introduce a layer of dimension reduction by a combination of Fourier analysis and low-rank matrix approximation. More specifically, we keep a large dimension representation from the Legendre projection to ensure that all the important details of historical data are preserved. We then apply a combination of Fourier analysis and low-rank approximation to keep the part of the representation related to low-frequency Fourier components and the top eigenspace to remove the impact of noises. We refer to the proposed method as Frequency Improved Legendre Memory model, or **FiLM** for short, for long-term time series forecasting.

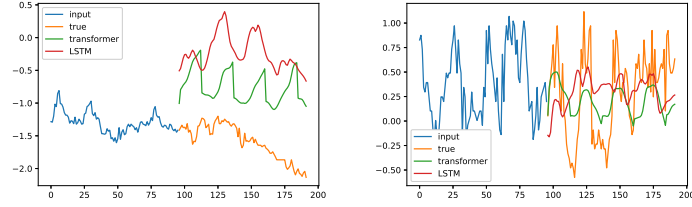


Figure 1: The discrepancy between ground truth and forecasting output from vanilla Transformer and LSTM on a real-world ETTh1 dataset Left: trend shift. Right: seasonal shift.

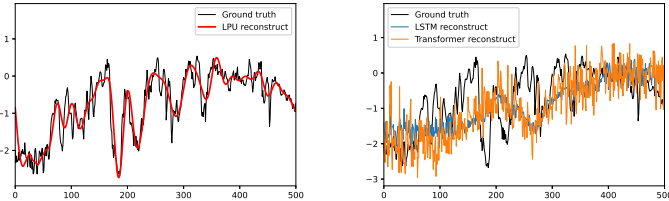


Figure 2: Data recovery with Autoencoder structure: recovery a 1024-length data with a bottleneck of 128 parameters. Left: Legendre Projection Unit. Right: LSTM and vanilla Transformer.

In short, we summarize the key contributions of this work as follows:

1. We propose a *Frequency improved Legendre Memory model* (FiLM) architecture with a mixture of experts for robust multiscale time series feature extraction.
2. We redesign the Legendre Projection Unit (LPU) and make it a general tool for data representation that any time series forecasting model can exploit to solve the historical information preserving problem.
3. We propose *Frequency Enhanced Layers* (FEL) that reduce dimensionality reduction by a combination of Fourier analysis and low-rank matrix approximation to minimize the impact of noisy signals from time series and ease the overfitting problem. The effectiveness of this method is verified both theoretically and empirically.
4. We conduct extensive experiments on six benchmark datasets across multiple domains (energy, traffic, economics, weather, and disease). Our empirical studies show that the proposed model improves the performance of state-of-the-art methods by **19.2%** and **26.1%** in multivariate and univariate forecasting, respectively. In addition, our empirical studies also reveal a dramatic improvement in computational efficiency through dimensionality reduction.

2 Time Series Representation in Legendre-Fourier Domain

2.1 Legendre Projection

Given an input sequence, the function approximation problem aims to approximate the cumulative history at every time t . Using Legendre function projection, we can project a prolonged sequence of data onto a subspace of bounded dimension, leading to compression, or feature representation, for evolving historical data. Formally, given a smooth function f observed online, we aim to maintain a fixed size compressed representation of its history $f(x)_{[t-\theta, t]}$, where θ specifies the window size.

At every time point t , the approximation function $g^{(t)}(x)$ is defined with respect to the measure $\mu^{(t)} = \frac{1}{\theta} \mathbb{I}_{[t-\theta, t]}(x)$. In this paper, we use Legendre polynomials of degree at most $N - 1$ to build the function $g^{(t)}(x)$, i.e.

$$g^{(t)}(x) = \sum_{n=1}^N c_n(t) P_n \left(\frac{2(x-t)}{\theta} + 1 \right), \quad (1)$$

where $P_n(\cdot)$ is the n -th order Legendre polynomial. Coefficients $c_n(t)$ are captured by the following dynamic equation

$$\frac{d}{dt} c(t) = -\frac{1}{\theta} A c(t) + \frac{1}{\theta} B f(t). \quad (2)$$

where the definition of A and B can be found in [Voelker et al. \(2019\)](#). Using Legendre polynomials as a basis allows us to accurately approximate smooth functions, as indicated by the following theorem.

Theorem 1 (*Similar to Proposition 6 in [Gu et al. \(2020\)](#)*). *If $f(x)$ is L -Lipschitz, then $\|f_{[t-\theta, t]}(x) - g^{(t)}(x)\|_{\mu^{(t)}} \leq \mathcal{O}(\theta L / \sqrt{N})$. Moreover, if $f(x)$ has k -th order bounded derivatives, we have $\|f_{[t-\theta, t]}(x) - g^{(t)}(x)\|_{\mu^{(t)}} \leq \mathcal{O}(\theta^k N^{-k+1/2})$.*

According to Theorem 1, without any surprise, the larger the number of Legendre polynomial basis, the more accurate the approximation will be, which unfortunately may lead to the overfitting of noisy signals in the history. As shown in Section 4, directly feeding deep learning modules, such as MLP, RNN, and vanilla attention without modification, with the above features will not yield state-of-the-art performance, primarily due to the noisy signals in history. That is why we introduce, in the following subsection, a frequency enhanced layer with Fourier transforms for feature selection.

Before we close this subsection, we note that unlike [Gu et al. \(2021a\)](#), a fixed window size is used for function approximation and feature extraction. This is largely because a longer history of data may lead to a larger accumulation of noises from history. To make it precise, we consider an auto-regressive setting with random noise. Let $\{x_t\} \in \mathbb{R}^d$ be the time sequence with $x_{t+1} = Ax_t + b + \epsilon_t$ for $t = 1, 2, \dots$, where $A \in \mathbb{R}^{d \times d}$, $b \in \mathbb{R}^d$, and $\epsilon_t \in \mathbb{R}^d$ is random noise sampled from $N(0, \sigma^2 I)$. As indicated by the following theorem, given x_t , the noise will accumulate in $x_{t-\theta}$ over time at the rate of $\sqrt{\theta}$, where θ is the window size.

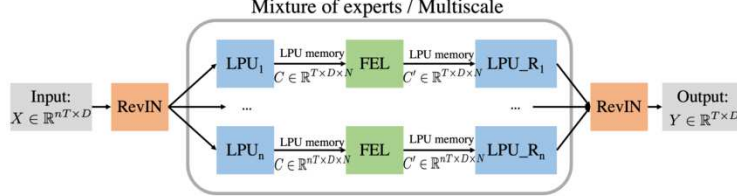


Figure 3: Overall structure of FiLM (Frequency improved Legendre Memory Model). LPU: Legendre Projection Unit. LPU_R: reverse recovery of Legendre Projection. FEL: Frequency Enhanced Layer. RevIn: data normalization block. The input data is first normalized and then project to Legendre Polynomial space (LPU memory C). The LPU memory C is processed with FEL and generates the memory C' of output. Finally, C' is reconstructed and denormalized to output series with LPU_R. A multiscale structure is employed to process the input with length $\{T, 2T, \dots, nT\}$.

Theorem 2. Let A be an unitary matrix and ϵ_t be σ^2 -subgaussian random noise. We have $x_t = A^\theta x_{t-\theta} + \sum_{i=1}^{\theta-1} A^i b + \mathcal{O}(\sigma\sqrt{\theta})$.

2.2 Fourier Transform

Because white noise has a completely flat power spectrum, it is commonly believed that the time series data enjoys a particular spectral bias, which is not generally randomly distributed in the whole spectrum. Due to the stochastic transition environment, the real output trajectories of the forecasting task contain large volatilities and people usually only predict the mean path of them. The relative more smooth solutions thus are preferred. According to Eq. (1), the approximation function $g^{(t)}(x)$ can be stabilized via smoothing the coefficients $c_n(t)$ in both t and n . This observation helps us design an efficient data-driven way to tune the coefficients $c_n(t)$. As smoothing in n can be simply implemented via multiplying learnable scalars to each channel, we mainly discuss smoothing $c_n(t)$ in t via Fourier transformation. The spectral bias implies the the spectrum of $c_n(t)$ mainly locates in low frequency regime and has weak signal strength in high frequency regime. To simplify our analysis, let us assume the Fourier coefficients of $c_n(t)$ as $a_n(t)$. Per spectral bias, we assume that there exists a $s, a_{\min} > 0$, such that for all n we have $t > s, |a_n(t)| \leq a_{\min}$. An idea to sample coefficients is to keep the the first k dimensions and randomly sample the remaining dimensions instead of the fully random sampling strategy. We characterize the approximation quality via the following theorem:

Theorem 3. Let $A \in \mathbb{R}^{d \times n}$ be the Fourier coefficients matrix of an input matrix $X \in \mathbb{R}^{d \times n}$, and $\mu(A)$, the coherence measure of matrix A , is $\Omega(k/n)$. We assume there exist s and a positive a_{\min} such that the elements in last $d - s$ columns of A is smaller than a_{\min} . If we keep first s columns selected and randomly choose $\mathcal{O}(k^2/\epsilon^2 - s)$ columns from the remaining parts, with high probability

$$\|A - P(A)\|_F \leq \mathcal{O} \left[(1 + \epsilon) a_{\min} \cdot \sqrt{(n - s)d} \right],$$

where $P(A)$ denotes the matrix projecting A onto the column selected column space.

Theorem 3 implies that when a_{\min} is small enough, the selected space can be considered as almost the same as the original ones.

3 Model Structure

3.1 FiLM: Frequency improved Legendre Memory Model

The overall structure of FiLM is shown in Figure 3. The FiLM maps a sequence $X \mapsto Y$, where $X, Y \in \mathbb{R}^{T \times D}$, by mainly utilizing two sub-layers: Legendre Projection Unit (LPU) layer and Fourier Enhanced Layer (FEL). In addition, to capture history information at different scales, a mixture of experts at different scales is implemented in the LPU layer. An optional add-on data normalization layer RevIN [Kim et al. \(2021\)](#) is introduced to enhance model robustness further. It is worth mentioning that FiLM is a simple model with only one layer of LPU and one layer of FEL.

LPU: Legendre Projection Unit LPU is a state space model: $C_t = AC_{t-1} + Bx_t$, where $x_t \in \mathbb{R}$ is the input signal, $C_t \in \mathbb{R}^N$ is the memory unit, and N is the number of Legendre Polynomial.

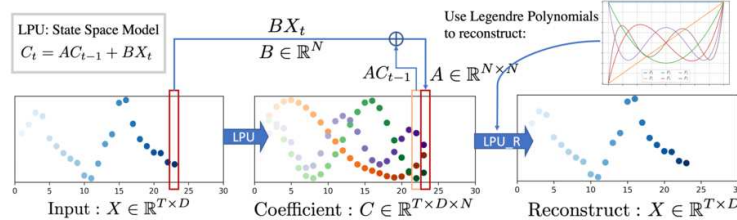


Figure 4: Structure of Legendre Projection Layer (LPU). LPU contains two states: Projection & Reconstruction. $C(t)$ is the compressed memory for decayed historical input up to time t . $x(t)$ is the original input signal at time t . A, B are two pre-fixed projection matrices. $C(t)$ is reconstructed to original input by multiplying a discrete Legendre Polynomial matrix.

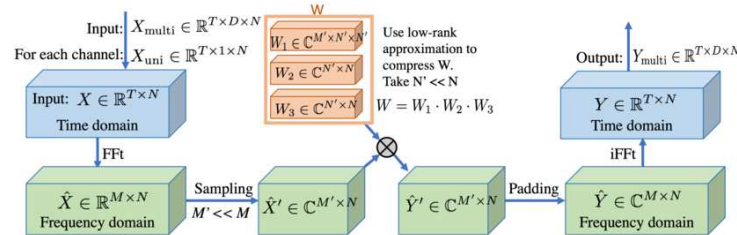


Figure 5: Structure of Frequency Enhanced Layer (FEL): Original version (use weights W) and Low-rank Approximation version (use weights $W = W_1 \cdot W_2 \cdot W_3$), where N is Legendre Polynomial number, M is Fourier mode number and T is sequence length.

LPU contains two untrainable prefixed matrices A and B defined as follows:

$$A_{nk} = (2n+1) \begin{cases} (-1)^{n-k} & \text{if } k \leq n \\ 1 & \text{if } k \geq n \end{cases}, B_n = (2n+1)(-1)^n. \quad (3)$$

LPU contains two stages, i.e., Projection and Reconstruction. The former stage projects the original signal to the memory unit: $C = \text{LPU}(X)$. The later stage reconstructs the signal from the memory unit: $X_{re} = \text{LPU_R}(C)$. The whole process in which the input signal is projected/reconstructed to/from memory C is shown in Figure 4.

FEL: Frequency Enhanced Layer

Low-rank Approximation The FEL is with a single learnable weight matrix ($W \in \mathbb{R}^{M' \times N \times N}$) which is all we need to learn from the data. However, this weight could be large. We can decompose W into three matrices $W_1 \in \mathbb{R}^{M' \times N' \times N'}$, $W_2 \in \mathbb{R}^{N' \times N}$ and $W_3 \in \mathbb{R}^{N' \times N}$ to perform a low-rank approximation. Take Legendre function number $N = 256$ as default, our model’s learnable weight can be significantly reduced to **0.4%** with $N' = 4$ with minor accuracy deterioration as shown in Section 4. The calculation mechanism is described in Figure 5.

Mode Selection A subset of the frequency modes is selected after Fourier transforms to reduce the noise. Our default selection policy is choosing the lowest M mode. Various selection policies are studied in the experiment section. Results show that adding some random high-frequency modes can give extra improvement in some datasets, as supported by our theoretical studies in Theorem 3.

Implementation source code for LPU and FEL are given in Appendix B.

3.2 Mixture of Multiscale Experts Mechanism

Multiscale phenomena is a unique critical data bias for time series forecasting. Since we treat history sequence points with uniform importance, our model might lack such prior. Our model implemented a simple mixture of experts strategy that utilizes the input sequence with various time horizons $\{T, 2T, \dots, nT\}$ to forecast the predicted horizon T and merge each expert prediction with linear layer as show in Figure 3. This mechanism improves the model’s performance consistently across all datasets, as shown in Table 7.

3.3 Data Normalization

As Wu et al. (2021); Zhou et al. (2022) point out, time series seasonal-trend decomposition is a crucial data normalization design for long-term time series forecasting. We find that our LMU projection can inherently play a normalization role for most datasets, but lacking an explicite normalization design still hurt the robustness of performance in some cases. A simple reversible instance normalization (RevIN) Kim et al. (2021) is adapted to act as a add-on explicite data normalization block. The mean and standard deviation are computed for every instance $x_k^{(i)} \in \mathbb{R}^T$ of the input data as $\mathbb{E}_t[x_{kt}^{(i)}] = \frac{1}{T} \sum_{j=1}^T x_{kj}^{(i)}$ and $\text{Var}[x_{kt}^{(i)}] = \frac{1}{T} \sum_{j=1}^T (x_{kj}^{(i)} - \mathbb{E}_t[x_{kt}^{(i)}])^2$. Using these statistics, we normalize the input data $x^{(i)}$ as $\hat{x}_{kt}^{(i)} = \gamma_k \left(\frac{x_{kt}^{(i)} - \mathbb{E}_t[x_{kt}^{(i)}]}{\sqrt{\text{Var}[x_{kt}^{(i)}] + \epsilon}} \right) + \beta_k$, where $\gamma, \beta \in \mathbb{R}^K$ are learnable affine parameter vectors. Then the normalized input data is sent into the model for forecasting. In the end, we denormalize the model output by applying the reciprocal of the normalization performed at the beginning.

RevIN slows down the training process by 2-5 times, and we do not observe consistent improvement on all datasets by applying RevIn. Thus, it can be considered an optional stabilizer in model training. Its detailed performance is shown in the ablation study in Table 7.

4 Experiments

Table 1: multivariate long-term series forecasting results on six datasets with input length $I = 96$ and prediction length $O \in \{96, 192, 336, 720\}$ (For ILI dataset, we use input length $I = 36$ and prediction length $O \in \{24, 36, 48, 60\}$). A lower MSE indicates better performance. All experiments are repeated 5 times.

Methods	FiLM		FEDformer		Autoformer		S4		Informer		LogTrans		Reformer		
	Metric	MSE	MAE	MSE	MAE	MSE	MAE	MSE	MAE	MSE	MAE	MSE	MAE	MSE	MAE
ET7 _{m2}	96	0.165	0.256	0.203	0.287	0.255	0.339	0.705	0.690	0.365	0.453	0.768	0.642	0.658	0.619
	192	0.222	0.296	0.269	0.328	0.281	0.340	0.924	0.692	0.533	0.563	0.989	0.757	1.078	0.827
	336	0.277	0.333	0.325	0.366	0.339	0.372	1.364	0.877	1.363	0.887	1.334	0.872	1.549	0.972
	720	0.371	0.389	0.421	0.415	0.422	0.419	0.877	1.074	3.379	1.338	3.048	1.328	2.631	1.242
Electricity	96	0.154	0.267	0.183	0.297	0.201	0.317	0.304	0.405	0.274	0.368	0.258	0.357	0.312	0.402
	192	0.164	0.258	0.195	0.308	0.222	0.334	0.313	0.413	0.296	0.386	0.260	0.368	0.348	0.433
	336	0.188	0.283	0.212	0.313	0.231	0.338	0.290	0.381	0.300	0.394	0.280	0.380	0.350	0.433
	720	0.236	0.332	0.231	0.343	0.254	0.361	0.262	0.344	0.373	0.439	0.283	0.376	0.340	0.420
Exchange	96	0.079	0.204	0.139	0.276	0.197	0.323	1.292	0.849	0.847	0.752	0.968	0.812	1.065	0.829
	192	0.159	0.292	0.256	0.369	0.300	0.369	1.631	0.968	1.204	0.895	1.040	0.851	1.188	0.906
	336	0.270	0.398	0.426	0.464	0.509	0.524	2.225	1.145	1.672	1.036	1.659	1.081	1.357	0.976
	720	0.830	0.721	1.090	0.800	1.447	0.941	2.521	1.245	2.478	1.310	1.941	1.127	1.510	1.016
Traffic	96	0.416	0.294	0.562	0.349	0.613	0.388	0.824	0.514	0.719	0.391	0.684	0.384	0.732	0.423
	192	0.408	0.288	0.562	0.346	0.616	0.382	1.106	0.672	0.696	0.379	0.685	0.390	0.733	0.420
	336	0.425	0.298	0.570	0.323	0.622	0.337	1.084	0.627	0.777	0.420	0.733	0.408	0.742	0.420
	720	0.520	0.353	0.596	0.368	0.660	0.408	1.536	0.845	0.864	0.472	0.717	0.396	0.755	0.423
Weather	96	0.199	0.262	0.217	0.296	0.266	0.336	0.406	0.444	0.300	0.384	0.458	0.490	0.689	0.596
	192	0.228	0.288	0.276	0.336	0.307	0.367	0.525	0.527	0.598	0.544	0.658	0.589	0.752	0.638
	336	0.267	0.323	0.339	0.380	0.359	0.395	0.531	0.539	0.578	0.523	0.797	0.652	0.639	0.596
	720	0.319	0.361	0.403	0.428	0.578	0.578	0.419	0.428	1.059	0.741	0.869	0.675	1.130	0.792
ILI	24	1.970	0.875	2.203	0.963	3.483	1.287	4.631	1.484	5.764	1.677	4.480	1.444	4.400	1.382
	36	1.982	0.859	2.272	0.976	3.103	1.148	4.123	1.348	4.755	1.467	4.799	1.467	4.783	1.448
	48	1.868	0.896	2.209	0.981	2.669	1.085	4.066	1.36	4.763	1.469	4.800	1.468	4.832	1.465
	60	2.057	0.929	2.545	1.061	2.770	1.125	4.278	1.41	5.264	1.564	5.278	1.560	4.882	1.483

To evaluate the proposed FiLM, we conduct extensive experiments on six popular real-world benchmark datasets for long-term forecasting, including traffic, energy, economics, weather, and disease. Since classic models such as ARIMA and simple RNN/TCN models perform inferior as shown in Zhou et al. (2021) and Wu et al. (2021), we mainly include five state-of-the-art (SOTA) Transformer-based models, i.e., FEDformer, Autoformer Wu et al. (2021), Informer Zhou et al. (2021), LogTrans Li et al. (2019), Reformer Kitaev et al. (2020), and one recent state-space model with recursive memory (S4 Gu et al. (2021a)), for comparison. FEDformer is selected as the main baseline as it achieves SOTA results in most settings. More details about baseline models, datasets, and implementations are described in Appendix C.

4.1 Main Result

For better comparison, we follow the experiment settings of Informer Zhou et al. (2021) where the input length is tuned for best forecasting performance, and the prediction lengths for both training and evaluation are fixed to be 96, 192, 336, and 720, respectively.

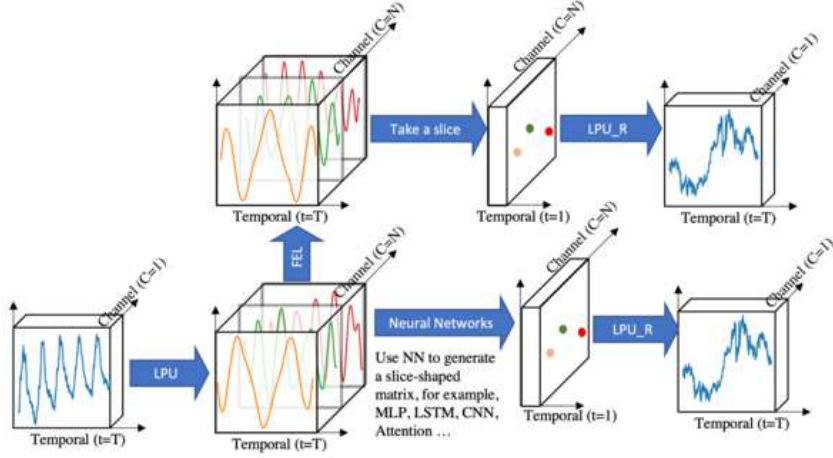


Figure 6: Legendre Projection Unit boosting effect. LPU can serve as a plug-in block in various backbones, e.g., FEL, MLP, LSTM, CNN, and Attention. Replacing LPU with comparable-sized linear layer will always lead to degraded performance.

Multivariate Results In multivariate forecasting tasks, FiLM achieves the best performance on all six benchmark datasets at all horizons, as shown in Table 1. Compared with SOTA work (FEDformer), our proposed FiLM yields an overall **19.2%** relative MSE reduction. It is worth noting that the improvement is even more significant on some of the datasets, such as Exchange (over 30%). The Exchange dataset does not exhibit apparent periodicity, but FiLM still achieves superior performance. Overall, the improvements made by FiLM are consistent with varying horizons, implying its strength in long-term forecasting. More detailed results on the ETT full benchmark are provided in Appendix C.5.

Univariate Results The benchmark results for univariate time series forecasting are summarized in Appendix C.4, Table 10. Compared with SOTA work (FEDformer), FiLM yields an overall **22.6%** relative MSE reduction. And on some datasets, such as Weather and Electricity, the improvement can reach more than 40%. It again demonstrates that FiLM is very effective in long-term forecasting.

LPU Boosting Results

A set of experiments are conducted to measure the boosting effect of LPU when combined with various common deep learning modules, as shown in Figure 6. It is worth mentioning that LPU does not contain any learnable parameters. The increasing of the model size does not result in such boosting effects. The results are shown in Table 2. For all the modules, LPU can be used to improve their average performance for long term time series forecasting significantly: MLP: **119.4%**, LSTM: **97.0%**, CNN: **13.8%**, Attention: **8.2%**. Vanilla Attention has a relative poor performance when combining the LPU which worth further digging.

Low-rank Approximation for FEL
 Low-rank approximation of learnable matrix in Frequency Enhanced Layer can significantly reduce our parameter size to **0.1%~0.4%** with minor accuracy deterioration. The experiment details are shown in Table 3. Compared to Transformer-based baselines, FiLM enjoys a lightweight

Table 2: Boosting effect of LPU layer for common deep learning backbones: MLP, LSTM, CNN and Attention. '+' indicates degraded performance

Methods	FiLM		MLP		LSTM		CNN		Attention		
	Compare	LPU	Linear	LPU	Linear	LPU	Linear	LPU	Linear	LPU	Linear
ETTIn1	96	0.030	+38%	0.034	+8.0%	0.049	+73%	0.116	-50%	0.243	-81%
	192	0.047	+9.5%	0.049	+30%	0.174	+52%	0.101	+20%	0.387	-86%
	336	0.063	+5.8%	0.061	+64%	0.119	+84%	0.122	+25%	1.652	+12%
	720	0.081	+1.4%	0.082	+62%	0.184	+32%	0.108	+13%	4.782	-61%
Electricity	96	0.213	+136%	0.431	+121%	0.291	+556%	0.310	+43%	0.805	+23%
	192	0.268	+32%	0.291	+239%	0.353	+17%	0.380	+12%	0.938	+14%
	336	0.307	+0.1%	0.296	+235%	0.436	-6.7%	0.359	+29%	2.043	-54%
	720	0.321	+37%	0.339	+196%	0.636	-11%	0.424	+18%	9.115	+298%

Table 3: Low-rank Approximation (LRA) study for Frequency Enhanced Layer (FEL): Comp. K=0 means default version without LRA, 1 means the largest compression using k=1

Comp. K	0		16		4		1		
	Metric	MSE	MAE	MSE	MAE	MSE	MAE	MSE	MAE
ETTIn1	96	0.371	0.394	0.371	0.396	0.371	0.398	0.400	0.421
	192	0.414	0.423	0.411	0.423	0.414	0.426	0.435	0.444
	336	0.442	0.445	0.443	0.446	0.443	0.444	0.492	0.478
	720	0.454	0.451	0.464	0.474	0.468	0.478	0.501	0.499
Weather	96	0.199	0.262	0.199	0.263	0.197	0.262	0.198	0.263
	192	0.228	0.288	0.225	0.285	0.226	0.285	0.225	0.286
	336	0.267	0.323	0.266	0.321	0.263	0.314	0.264	0.316
	720	0.319	0.361	0.314	0.355	0.315	0.354	0.318	0.357
Parameter Size		100%		1.95%		0.41%		0.10%	

property with **80%** learnable parameter reductions as shown in Appendix **G**.

Mode selection policy for FEL Frequency mode selection policy is studied in Table 4. The *Lowest* mode selection method shows the most robust performance. The results in *Low random* column shows that randomly adding some high-frequency info gives extra improvement in some datasets, as our theoretical studies in Theorem 3 support.

4.2 Ablation Study

This subsection summarizes the ablation study, especially the effectiveness of the two major blocks (FEL & LPU) employed.

Table 4: Mode selection policy study for frequency enhanced layer: Lowest: select the lowest m frequency mode, random: select M random frequency mode. 3. low random: select the $0.8* M$ lowest frequency mode and $0.2* M$ random high frequency mode.

Policy	Lowest		Random		Low random		
	Metric	MSE	MAE	MSE	MAE	MSE	MAE
Exchange	96	0.079	0.204	0.083	0.208	0.087	0.210
	192	0.159	0.292	0.187	0.318	0.207	0.340
	336	0.270	0.398	0.271	0.395	0.353	0.461
	720	0.788	0.680	0.788	0.680	0.748	0.674
Weather	96	0.199	0.262	0.197	0.256	0.196	0.254
	192	0.228	0.288	0.234	0.300	0.234	0.301
	336	0.267	0.323	0.266	0.319	0.263	0.316
	720	0.319	0.361	0.317	0.356	0.316	0.354

Table 5: Ablation studies of LPU layer. The original LPU block (whose projection and reconstruction matrix are fixed) is replaced with 6 variants (**Fixed** means the matrix are not trainable. **Trainable** means the matrix is initialized with original parameters and trainable. **Random Init** means the matrix is initialized randomly and trainable). The experiments are performed on ETTm1 and Electricity with different input lengths. The metric of variants is presented in relative value (‘+’ indicates degraded performance, ‘-’ indicates improved performance).

Index	Original		Variant 1		Variant 2		Variant 3		Variant 4		Variant 5		Variant 6	
	Projection	Reconstruction	Fixed	Trainable	Fixed	Trainable	Fixed	Trainable	Random Init	Linear	Random Init	Linear	MSE	MAE
ETTm1	Metric		MSE	MAE	MSE	MAE	MSE	MAE	MSE	MAE	–	–	MSE	MAE
	96	0.030	0.128	+6.0%	+3.1%	+4.6%	+3.1%	+4.7%	+2.7%	+0.7%	+0.6%	NaN	+38%	+22%
	192	0.047	0.160	-2.6%	-1.3%	+2.5%	+1.8%	-0.4%	+0.4%	-3.0%	-1.0%	NaN	+9.5%	+8.7%
	336	0.063	0.185	+4.2%	+1.8%	-2.4%	-0.4%	-6.3%	-2.5%	+2.2%	+1.4%	NaN	+5.8%	+5.0%
Electricity	720	0.081	0.215	-0.4%	-0.6%	+24%	+12%	+11%	+5.9%	NaN	NaN	NaN	+1.4%	+2.2%
	96	0.213	0.328	+15%	+6.8%	+11%	+5.2%	+11%	+5.1%	+11%	+4.8%	NaN	+136%	+58%
	192	0.268	0.373	-4.6%	-3.8%	+7.8%	+3.9%	+6.8%	+3.5%	-5.3%	-3.9%	NaN	+32%	+16%
	336	0.307	0.417	-4.2%	-5.0%	-3.9%	-6.0%	-7.2%	-8.0%	-8.5%	-9.0%	NaN	+0.1%	-5.0%
	720	0.321	0.423	+2.9%	+2.8%	+10%	+6.8%	+3.0%	+1.7%	+207%	+85%	NaN	37%	22%

Efficiency of LPU To prove the effectiveness of LPU layer, in Table 5, we compare the original LPU layer with six variants. The LPU layer consists of two sets of matrices (Projection matrices & Reconstruction matrices). Each has three variants: Fixed, Trainable, and Random Init. In Variant 6, we use comparable-sized linear layers to replace the LPU layer. We observe that Variant 6 leads to a 32.5% degradation on average, which confirms the effectiveness of Legendre projection. The projection matrix in LPU is called N times recursively (N is the input length). So if the projection matrix is randomly initited (Variant 5), the output will face the problem of exponential explosion. If the projection matrix is trainable (Variants 2, 3, 4), the model suffers from the exponential explosion as well and thus needs to be trained with a small learning rate, which leads to a plodding training speed requiring more epochs for convergence. Thus, the trainable projection version is not recommended, considering the trade-off between speed and performance. The variant trainable reconstruction matrix (Variant 1) has comparable performance and less difficulty in convergence.

Efficiency of FEL To prove the effectiveness of the FEL, we replace the FEL with multiple variants (MLP, LSTM, CNN, and Transformer). S4 is also introduced as a variant since it has a version with Legendre projection memory. The experimental results are summarized in Table 6. FEL achieves the best performance and has more than 100% improvement on average compared with its LSTM, CNN, and Attention counterpart. MLP has comparable performance when input length is 192, 336, and 720. However, MLP suffers from insupportable memory usage, which is $N^2 L$ (while FEL is N^2). S4 achieves similar results as our LPU+MLP variant. Among all, the LPU+vanilla Attention variant shows the poorest performance.

Efficiency of Multiscale and Normalization The multiscale module leads to significant improvement on all datasets consistently. However, the data normalization achieves mixed performance,

Table 6: Ablation studies of FEL layer. The FEL layer is replaced with 4 different variants: MLP, LSTM, CNN, and Transformer. S4 is also introduced as a variant. The experiments are performed on ETTm1 and Electricity. The metric of variants is presented in relative value ('+' indicates degraded performance, '-' indicates improved performance).

Methods	FiLM		LPU+MLP		LPU+LSTM		LPU+CNN		LPU+attention		S4	
Metric	MSE	MAE	MSE	MAE	MSE	MAE	MSE	MAE	MSE	MAE	MSE	MAE
ETTm1	96	0.030	0.128	+14%	+6.6%	+62%	+31%	+286%	+118%	+709%	+166%	-
	192	0.047	0.160	+3.8%	+2.2%	+271%	+122%	+116%	+58%	+727%	+136%	-
	336	0.063	0.185	-3.7%	-2.1%	+90%	+51%	+94%	+48%	+2524%	+286%	-
	720	0.081	0.215	+0.9%	-0.6%	+127%	+65%	+33%	+17%	+5783%	+299%	-
Electricity	96	0.213	0.328	+103%	+40%	+37%	+20%	+46%	+23%	+278%	+105%	65% 38%
	192	0.268	0.373	+8.7%	+0.01%	+32%	+14%	+42%	+21%	+249%	+81%	39% 22%
	336	0.307	0.417	-3.7%	-8.5%	+42%	+13%	+17%	+6.0%	+564%	+90%	33% 15%
	720	0.321	0.423	+5.7%	+1.4%	+98%	+36%	+32%	+18%	+2739%	+117%	47% 22%

Table 7: Ablation studies of Normalization and Multiscale. Multiscale use 3 branches with: T , $2T$, and $4T$ as input sequence length. T is the predicted sequence length

Dataset	ETTm2		Electricity		Exchange		Traffic		Weather		Illness	
Metric	MSE	Relative	MSE	Relative	MSE	Relative	MSE	Relative	MSE	Relative	MSE	Relative
Methods	Original	0.301	+16%	0.195	+4.8%	0.534	+ 60%	0.528	+19%	0.264	+4.9%	3.55 + 80%
	Normalization	0.268	+3.6%	0.199	+6.4%	0.456	+36%	0.656	+48%	0.256	+1.5%	3.36 +70%
	Multiscale	0.259	+ 0.19%	0.187	+0%	0.335	0%	0.541	+22%	0.253	+0.50%	2.41 +22%
	With both	0.271	+4.7%	0.189	+1.5%	0.398	+19%	0.442	+0%	0.253	+0.4%	1.97 +0%

leading to improved performance on Traffic and Illness but a slight improvement on the rest. The Ablation study of RevIN data normalization and the mixture of multiscale experts employed is shown in Table 7.

4.3 Other Studies

Other supplemental studies are provided in Appendix. 1. A parameter sensitivity experiment (in Appendix D) is carried out to discuss the choice of hyperparameter for M and N, where M is the frequency mode number and N is the Legendre Polynomial number. 2. A noise injection experiment (in Appendix E) is conducted to show the robustness of our model. 3. A Kolmogorov-Smirnov test (in Appendix F) is conducted to discuss the similarity between the output distribution and the input. Our proposed FiLM has the best similarity, which supports our model design. 4. At last, (in Appendix H), we show that our model has a good linear time and memory usage.

5 Discussions and Conclusion

In long-term forecasting, the critical challenge is the trade-off between historical information preservation and noise reduction for accurate and robust forecasting. To address this challenge, we propose a Frequency improved Legendre Memory model, or **FiLM**, to preserve historical information accurately and remove noisy signals. Moreover, we theoretically and empirically prove the effectiveness of the Legendre and Fourier projection employed in our model. Extensive experiments show that the proposed model achieves SOTAaccuracy by a significant margin on six benchmark datasets. In particular, we would like to point out that our proposed framework is rather general and can be used as the building block for long-term forecasting in future research. It can be modified for different scenarios. For example, the Legendre Projection Unit can be replaced with other orthogonal functions such as Laguerre, Fourier, and Chebyshev polynomials, etc. In addition, based on the properties of noises, modules other than Fourier Enhanced Layer can be plugged into the framework. We plan to investigate more variants and more underlying insights into this framework in the future.

References

Box, G. E. P. and Jenkins, G. M. Some recent advances in forecasting and control. *Journal of the Royal Statistical Society. Series C (Applied Statistics)*, 17(2):91–109, 1968.

Box, G. E. P. and Pierce, D. A. Distribution of residual autocorrelations in autoregressive-integrated moving average time series models. volume 65, pp. 1509–1526. Taylor & Francis, 1970.

Choromanski, K. M., Likhoshesterov, V., Dohan, D., Song, X., Gane, A., Sarlós, T., Hawkins, P., Davis, J. Q., Mohiuddin, A., Kaiser, L., Belanger, D. B., Colwell, L. J., and Weller, A. Rethinking attention with performers. In *9th International Conference on Learning Representations (ICLR), Virtual Event, Austria, May 3-7, 2021*, 2021.

Chung, J., Gülcöhre, C., Cho, K., and Bengio, Y. Empirical evaluation of gated recurrent neural networks on sequence modeling. *CoRR*, abs/1412.3555, 2014.

Devlin, J., Chang, M., Lee, K., and Toutanova, K. BERT: pre-training of deep bidirectional transformers for language understanding. In *Proceedings of the 2019 Conference of the North American Chapter of the Association for Computational Linguistics: Human Language Technologies (NAACL-HLT), Minneapolis, MN, USA, June 2-7, 2019*, pp. 4171–4186, 2019.

Dosovitskiy, A., Beyer, L., Kolesnikov, A., Weissenborn, D., Zhai, X., Unterthiner, T., Dehghani, M., Minderer, M., Heigold, G., Gelly, S., Uszkoreit, J., and Houlsby, N. An image is worth 16x16 words: Transformers for image recognition at scale. In *9th International Conference on Learning Representations, ICLR 2021, Virtual Event, Austria, May 3-7, 2021*, 2021.

Gu, A., Dao, T., Ermon, S., Rudra, A., and Ré, C. Hippo: Recurrent memory with optimal polynomial projections. *Advances in Neural Information Processing Systems*, 33:1474–1487, 2020.

Gu, A., Goel, K., and Ré, C. Efficiently modeling long sequences with structured state spaces. *arXiv preprint arXiv:2111.00396*, 2021a.

Gu, A., Johnson, I., Goel, K., Saab, K., Dao, T., Rudra, A., and Ré, C. Combining recurrent, convolutional, and continuous-time models with linear state space layers. *Advances in Neural Information Processing Systems*, 34, 2021b.

Gupta, G., Xiao, X., and Bogdan, P. Multiwavelet-based operator learning for differential equations. In *Advances in Neural Information Processing Systems (NeurIPS), 2021, December 6-14, 2021, virtual*, pp. 24048–24062, 2021.

Hochreiter, S. and Schmidhuber, J. Long short-term memory. *Neural computation*, 9(8):1735–1780, 1997a.

Hochreiter, S. and Schmidhuber, J. Long Short-Term Memory. *Neural Computation*, 9(8):1735–1780, November 1997b. ISSN 0899-7667, 1530-888X.

Kim, T., Kim, J., Tae, Y., Park, C., Choi, J.-H., and Choo, J. Reversible instance normalization for accurate time-series forecasting against distribution shift. In *International Conference on Learning Representations*, 2021.

Kingma, D. P. and Ba, J. Adam: A Method for Stochastic Optimization. *arXiv:1412.6980 [cs]*, January 2017. arXiv: 1412.6980.

Kitaev, N., Kaiser, L., and Levskaya, A. Reformer: The efficient transformer. In *8th International Conference on Learning Representations, ICLR 2020, Addis Ababa, Ethiopia, April 26-30, 2020*, 2020.

Lai, G., Chang, W.-C., Yang, Y., and Liu, H. Modeling long-and short-term temporal patterns with deep neural networks. In *The 41st International ACM SIGIR Conference on Research & Development in Information Retrieval*, pp. 95–104, 2018.

Lee-Thorp, J., Ainslie, J., Eckstein, I., and Ontañón, S. FNet: Mixing tokens with fourier transforms. *CoRR*, abs/2105.03824, 2021.

Li, S., Jin, X., Xuan, Y., Zhou, X., Chen, W., Wang, Y.-X., and Yan, X. Enhancing the locality and breaking the memory bottleneck of transformer on time series forecasting. In *Advances in Neural Information Processing Systems*, volume 32, 2019.

Li, Z., Kovachki, N. B., Azizzadenesheli, K., Liu, B., Bhattacharya, K., Stuart, A. M., and Anandkumar, A. Fourier neural operator for parametric partial differential equations. *CoRR*, abs/2010.08895, 2020.

Ma, X., Kong, X., Wang, S., Zhou, C., May, J., Ma, H., and Zettlemoyer, L. Luna: Linear unified nested attention. *CoRR*, abs/2106.01540, 2021.

Pascanu, R., Mikolov, T., and Bengio, Y. On the difficulty of training recurrent neural networks. In *Proceedings of the 30th International Conference on Machine Learning, ICML 2013, Atlanta, GA, USA, 16-21 June 2013*, volume 28, pp. 1310–1318, 2013.

Paszke, A., Gross, S., Massa, F., Lerer, A., Bradbury, J., Chanan, G., Killeen, T., Lin, Z., Gimelshein, N., Antiga, L., Desmaison, A., Kopf, A., Yang, E., DeVito, Z., Raison, M., Tejani, A., Chilamkurthy, S., Steiner, B., Fang, L., Bai, J., and Chintala, S. Pytorch: An imperative style, high-performance deep learning library. In *Advances in Neural Information Processing Systems*, pp. 8024–8035. 2019.

Qin, Y., Song, D., Chen, H., Cheng, W., Jiang, G., and Cottrell, G. W. A dual-stage attention-based recurrent neural network for time series prediction. In *Proceedings of the Twenty-Sixth International Joint Conference on Artificial Intelligence (IJCAI), Melbourne, Australia, August 19-25, 2017*, pp. 2627–2633. ijcai.org, 2017.

Qiu, J., Ma, H., Levy, O., Yih, W., Wang, S., and Tang, J. Blockwise self-attention for long document understanding. In *Findings of the Association for Computational Linguistics: EMNLP 2020, Online Event, 16-20 November 2020*, volume EMNLP 2020 of *Findings of ACL*, pp. 2555–2565. Association for Computational Linguistics, 2020.

Rangapuram, S. S., Seeger, M. W., Gasthaus, J., Stella, L., Wang, Y., and Januschowski, T. Deep state space models for time series forecasting. In *Advances in Neural Information Processing Systems*, volume 31, 2018.

Rao, Y., Zhao, W., Zhu, Z., Lu, J., and Zhou, J. Global filter networks for image classification. *Advances in Neural Information Processing Systems*, 34, 2021.

Salinas, D., Flunkert, V., Gasthaus, J., and Januschowski, T. DeepAR: Probabilistic forecasting with autoregressive recurrent networks. *International Journal of Forecasting*, 36(3):1181–1191, 2020.

Sen, R., Yu, H., and Dhillon, I. S. Think globally, act locally: A deep neural network approach to high-dimensional time series forecasting. In *Advances in Neural Information Processing Systems (NeurIPS), December 8-14, 2019, Vancouver, BC, Canada*, pp. 4838–4847, 2019.

Tay, Y., Bahri, D., Yang, L., Metzler, D., and Juan, D. Sparse sinkhorn attention. In *Proceedings of the 37th International Conference on Machine Learning, ICML 2020, 13-18 July 2020, Virtual Event*, volume 119 of *Proceedings of Machine Learning Research*, pp. 9438–9447. PMLR, 2020a.

Tay, Y., Dehghani, M., Abnar, S., Shen, Y., Bahri, D., Pham, P., Rao, J., Yang, L., Ruder, S., and Metzler, D. Long range arena: A benchmark for efficient transformers. *arXiv preprint arXiv:2011.04006*, 2020b.

Vaswani, A., Shazeer, N., Parmar, N., Uszkoreit, J., Jones, L., Gomez, A. N., Kaiser, Ł., and Polosukhin, I. Attention is all you need. *Advances in neural information processing systems*, 30, 2017.

Voelker, A., Kajić, I., and Eliasmith, C. Legendre memory units: Continuous-time representation in recurrent neural networks. In *Advances in Neural Information Processing Systems*, volume 32, 2019.

Wang, J., Wang, Z., Li, J., and Wu, J. Multilevel wavelet decomposition network for interpretable time series analysis. In *Proceedings of the 24th ACM SIGKDD International Conference on Knowledge Discovery & Data Mining*, pp. 2437–2446, 2018.

Wang, S., Li, B. Z., Khabsa, M., Fang, H., and Ma, H. Linformer: Self-attention with linear complexity. *CoRR*, abs/2006.04768, 2020.

Wen, Q., Zhou, T., Zhang, C., Chen, W., Ma, Z., Yan, J., and Sun, L. Transformers in time series: A survey. *arXiv preprint arXiv:2202.07125*, 2022.

Wu, H., Xu, J., Wang, J., and Long, M. Autoformer: Decomposition transformers with auto-correlation for long-term series forecasting. In *Proceedings of the Advances in Neural Information Processing Systems (NeurIPS)*, pp. 101–112, 2021.

Xiong, Y., Zeng, Z., Chakraborty, R., Tan, M., Fung, G., Li, Y., and Singh, V. Nyströmformer: A nyström-based algorithm for approximating self-attention. In *Thirty-Fifth AAAI Conference on Artificial Intelligence*, pp. 14138–14148, 2021.

Zhang, J., Lin, Y., Song, Z., and Dhillon, I. S. Learning long term dependencies via fourier recurrent units. In *Proceedings of the 35th International Conference on Machine Learning (ICML), Stockholmsmässan, Stockholm, Sweden, July 10-15, 2018*, volume 80, pp. 5810–5818, 2018.

Zhou, H., Zhang, S., Peng, J., Zhang, S., Li, J., Xiong, H., and Zhang, W. Informer: Beyond efficient transformer for long sequence time-series forecasting. In *The Thirty-Fifth AAAI Conference on Artificial Intelligence, AAAI 2021, Virtual Conference*, volume 35, pp. 11106–11115, 2021.

Zhou, T., Ma, Z., Wen, Q., Wang, X., Sun, L., and Jin, R. FEDformer: Frequency enhanced decomposed transformer for long-term series forecasting. In *39th International Conference on Machine Learning (ICML)*, 2022.

Zhu, Z. and Soricut, R. H-transformer-1d: Fast one-dimensional hierarchical attention for sequences. In *Proceedings of the 59th Annual Meeting of the Association for Computational Linguistics (ACL) 2021, Virtual Event, August 1-6, 2021*, pp. 3801–3815, 2021.

A Related Work

In this section, an overview of the literature for time series forecasting will be given.

Traditional Time Series Models The first generation of well-discussed time series model is the autoregressive family. ARIMA [Box & Jenkins \(1968\)](#); [Box & Pierce \(1970\)](#) follows the Markov process and build recursive sequential forecasting. However, an autoregressive process has difficulty in dealing non-stationary sequences. Thus, ARIMA employed a pre-process iteration by differencing, which transforms the series to stationary.

Deep Neural Network in Forecasting With the bloom of deep neural networks, recurrent neural networks (RNN) was designed for tasks involving sequential data. However, canonical RNN tends to suffer from gradient vanishing/exploding problem with long input because of its recurrent structure. Among the family of RNNs, LSTM [Hochreiter & Schmidhuber \(1997b\)](#) and GRU [Chung et al. \(2014\)](#) proposed gated structure to control the information flow to deal with the gradient vanishing/exploration problem. Although recurrent networks enjoys fast inference, they are slow to train and not parallelizable. Temporal convolutional network (TCN) [Sen et al. \(2019\)](#) is another family for sequential tasks. However, limited to the reception field of the kernel, the long-term dependencies are hard to grasp. Convolution is a parallelizable operation but expensive in inference.

Efficient Transformers With the innovation of transformers in natural language processing [Vaswani et al. \(2017\)](#); [Devlin et al. \(2019\)](#) and computer vision tasks [Dosovitskiy et al. \(2021\)](#); [Rao et al. \(2021\)](#), transformer-based models are also discussed, renovated, and applied in time series forecasting [Zhou et al. \(2021\)](#); [Wu et al. \(2021\)](#). Some works use temporal attention [Qin et al. \(2017\)](#) to capture long-range dependencies. Others use the backbone of Transformer. Transformers usually employs an encoder-decoder architecture, with the self-attention and cross-attention mechanisms serving as the core layers. However, when employing a point-wise connected attention mechanism, the transformers suffer from quadratic computation complexity.

To get efficient computation without sacrificing too much on performance, the earliest modifications specify the attention matrix with predefined patterns. Examples include: [Qiu et al. \(2020\)](#) uses block-wise attention which reduces the complexity to the square of block size. LogTrans [Li et al. \(2019\)](#) uses log-sparse attention and achieves $N \log^2 N$ complexity. H-transformer [Zhu & Soricut \(2021\)](#) uses a hierarchical pattern for sparse approximation of attention matrix with $O(n)$ complexity. Another strategy is to use dynamic patterns: Reformer [Kitaev et al. \(2020\)](#) introduces a local-sensitive hashing which reduces the complexity to $N \log N$. [Zhu & Soricut \(2021\)](#) introduces a hierarchical pattern. Sinkhorn [Tay et al. \(2020a\)](#) employs a block sorting method to achieve quasi-global attention with only local windows.

Similarly, some work employs a top-k truncating to accelerate computing: Informer [Zhou et al. \(2021\)](#) uses a KL-divergence based method to select top-k in attention matrix. This sparser matrix costs only $N \log N$ in complexity. Autoformer [Wu et al. \(2021\)](#) introduces an auto-correlation block in place of canonical attention to get the sub-series level attention, which achieves $N \log N$ complexity.

Another emerging strategy is to employ a low-rank approximation of the attention matrix. Linformer [Wang et al. \(2020\)](#) uses trainable linear projection to compress the sequence length and achieves $O(n)$ complexity and theoretically proves the boundary of approximation error based on JL lemma. Luna [Ma et al. \(2021\)](#) develops a nested linear structure with $O(n)$ complexity. Nyströmformer [Xiong et al. \(2021\)](#) leverages the idea of Nyström approximation in the attention mechanism and achieves an $O(n)$ complexity. Performer [Choromanski et al. \(2021\)](#) adopts an orthogonal random features approach to efficiently model kernelizable attention mechanisms.

Orthogonal Basis and Neural Network Orthogonal basis project arbitrary functions onto a certain space and thus enable the representation learning in another view. Orthogonal basis family is easy to be discretized and to serve as an plug-in operation in neural networks. Recent studies began to realize the efficiency and effectiveness of Orthogonal basis, including the Polynomial family and others (Fourier basis & Multiwavelet basis). Fourier basis is first introduced for acceleration due to Fast Fourier algorithm, for example, acceleration of computing convolution [Gu et al. \(2020\)](#) or Auto-correlation function [Wu et al. \(2021\)](#). Fourier basis also serves as a performance boosting block:

Fourier with Recurrent structure [Zhang et al. \(2018\)](#), Fourier with MLP [Li et al. \(2020\)](#); Lee-Thorp [et al. \(2021\)](#) and Fourier in Transformer [Zhou et al. \(2022\)](#). Multiwavelet transform is a more local filter (compared with Fourier) and a frequency decomposer. Thus, neural networks which employ multiwavelet filter usually exhibit a hierarchical structure and treat different frequency in different tunnels, for example, [Wang et al. \(2018\)](#); [Gupta et al. \(2021\)](#); [Zhou et al. \(2022\)](#). Orthogonal Polynomials are naturally good selections of orthogonal basis. Legendre Memory Unit (LMU) [Voelker et al. \(2019\)](#) uses Legendre Polynomials for an orthogonal projection of input signals for a memory strengthening with the backbone of LSTM. The projection process is mathematically derived from delayed linear transfer function. HiPPO [Gu et al. \(2020\)](#), based on LMU, proposes a novel mechanism (Scaled Legendre), which involves the function’s full history (LMU uses decayed memory). In the subsequent work of HiPPO, the authors propose S4 [Gu et al. \(2021a\)](#) model and gives the first practice on time series forecasting tasks. However, LMU and HiPPO shared the same backbone (LSTM), which may limit their performance. Furthermore, the setting of Scale Legendre in HiPPO (history without decay) may not stand in time series forecasting.

B Algorithm Implementation

Algorithm 1 Frequency Enhanced Layer

```

class Freq_enhanced_layer(nn.Module):
    def __init__(self, in_channels, out_channels, modes1, compression=0):
        super(Freq_enhanced_layer, self).__init__()
        self.in_channels = in_channels
        self.out_channels = out_channels
        self.modes1 = modes1 #Number of Fourier modes to multiply, at most floor(N/2) + 1
        self.compression= compression
        self.scale = (1 / (in_channels*out_channels))
        self.weights1 = nn.Parameter(self.scale * torch.rand(in_channels, out_channels, self.modes1))
        if compression>0: ## Low-rank approximation
            self.weights0 = nn.Parameter(self.scale * torch.rand(in_channels, self.compression, dtype=
                torch.cfloat))
            self.weights1 = nn.Parameter(self.scale * torch.rand(self.compression, self.compression, len(
                self.index), dtype=torch.cfloat))
            self.weights2 = nn.Parameter(self.scale * torch.rand(self.compression, out_channels, dtype=
                torch.cfloat))

    def forward(self, x):
        B, H, E, N = x.shape
        # Compute Fourier coefficients up to factor of e^(- something constant)
        x_ft = torch.fft.rfft(x)
        # Multiply relevant Fourier modes
        out_ft = torch.zeros(B,H, self.out_channels, x.size(-1)//2 + 1)
        if self.compression==0:
            a = x_ft[:, :, :, :self.modes1]
            out_ft[:, :, :, :self.modes1] = torch.einsum("bjix,iox->bjox", a, self.weights1)
        else:
            a = x_ft[:, :, :, :self.modes2]
            a = torch.einsum("bjix,ih->jhx", a, self.weights0)
            a = torch.einsum("bjhx,hkx->bjkx", a, self.weights1)
            out_ft[:, :, :, :self.modes2] = torch.einsum("bjkx,ko->bjox", a, self.weights2)
        # Return to physical space
        x = torch.fft.irfft(out_ft, n=x.size(-1))
        return x

```

C Dataset and Implementation Details

C.1 Dataset Details

In this paragraph, the details of the experiment datasets are summarized as follows: 1) ETT [Zhou et al. \(2021\)](#) dataset contains two sub-dataset: ETT1 and ETT2, collected from two electricity transformers. Each of them has two versions with different resolutions (15min & 1h). ETT dataset contains multiple series of loads and one series of oil temperatures. 2) Electricity¹ dataset contains the electricity consumption of clients with each column corresponding to one client. 3) Exchange [Lai et al. \(2018\)](#) dataset contains the current exchange of 8 countries. 4) Traffic² dataset contains the

¹<https://archive.ics.uci.edu/ml/datasets/ElectricityLoadDiagrams 20112014>

²<http://pems.dot.ca.gov>

Algorithm 2 LPU layer

```
from scipy import signal
from scipy import special as ss
class LPU(nn.Module):
    def __init__(self, N=256, dt=1.0, discretization='bilinear'):
        # N: the order of the Legendre projection
        # dt: step size - can be roughly inverse to the length of the sequence
        super(LPU, self).__init__()
        self.N = N
        A, B = transition(N) ### LPU projection matrix
        A, B, _, _, _ = signal.cont2discrete((A, B, C, D), dt=dt, method=discretization)
        B = B.squeeze(-1)
        self.register_buffer('A', torch.Tensor(A))
        self.register_buffer('B', torch.Tensor(B))
    def forward(self, inputs):
        # inputs: (length, ...)
        # output: (length, ..., N) where N is the order of the Legendre projection
        c = torch.zeros(inputs.shape[:-1] + tuple([self.N]))
        cs = []
        for f in inputs.permute([-1, 0, 1]):
            f = f.unsqueeze(-1)
            new = f @ self.B.unsqueeze(0) # [B, D, H, 256]
            c = F.linear(c, self.A) + new
            cs.append(c)
        return torch.stack(cs, dim=0)
    def reconstruct(self, c):
        a = (self.eval_matrix @ c.unsqueeze(-1)).squeeze(-1)
        return (self.eval_matrix @ c.unsqueeze(-1)).squeeze(-1)
```

Table 8: Summarized feature details of six datasets.

DATASET	LEN	DIM	FREQ
ETTM2	69680	8	15 MIN
ELECTRICITY	26304	322	1H
EXCHANGE	7588	9	1 DAY
TRAFFIC	17544	863	1H
WEATHER	52696	22	10 MIN
ILI	966	8	7 DAYS

occupation rate of freeway system across the State of California. 5) Weather³ dataset contains 21 meteorological indicators for a range of 1 year in Germany. 6) Illness⁴ dataset contains the influenza-like illness patients in the United States. Table 8 summarizes feature details (Sequence Length: Len, Dimension: Dim, Frequency: Freq) of the six datasets. All datasets are split into the training set, validation set and test set by the ratio of 7:1:2.

C.2 Implementation Details

Our model is trained using ADAM Kingma & Ba (2017) optimizer with a learning rate of $1e^{-4}$. The batch size is set to 32 (In fact, a batch size up to 256 will not deteriorate the performance but with faster training speed). An early stopping counter is employed to stop the training process after three epochs if no loss degradation on the valid set is observed. The mean square error (MSE) and mean absolute error (MAE) are used as metrics. All experiments are repeated 5 times and the mean of the metrics is used in the final results. All the deep learning networks are implemented in PyTorch Paszke et al. (2019) and trained on NVIDIA V100 32GB GPUs.

C.3 Experiments Error Bars

We train our model 5 times and calculate the error bars for FiLM and SOTA model FEDformer to show the robustness of our proposed model.

C.4 Univariate Forecasting Result Table

The univariate benchmark is shown in Table 10.

³<https://www.bgc-jena.mpg.de/wetter/>

⁴<https://gis.cdc.gov/grasp/fluvview/fluportaldashboard.html>

Table 9: MSE with error bars (Mean and STD) for FiLM and FEDformer baseline for multivariate long-term forecasting.

	MSE	ETTm2	Electricity	Exchange	Traffic
FiLM	96	0.165 ± 0.0051	0.153 ± 0.0014	0.079 ± 0.002	0.416 ± 0.010
	192	0.222 ± 0.0038	0.165 ± 0.0023	0.159 ± 0.011	0.408 ± 0.007
	336	0.277 ± 0.0021	0.186 ± 0.0018	0.270 ± 0.018	0.425 ± 0.007
	720	0.371 ± 0.0066	0.236 ± 0.0022	0.788 ± 0.026	0.520 ± 0.003
FED-f	96	0.203 ± 0.0042	0.194 ± 0.0008	0.148 ± 0.002	0.217 ± 0.008
	192	0.269 ± 0.0023	0.201 ± 0.0015	0.270 ± 0.008	0.604 ± 0.004
	336	0.325 ± 0.0015	0.215 ± 0.0018	0.460 ± 0.016	0.621 ± 0.006
	720	0.421 ± 0.0038	0.246 ± 0.0020	1.195 ± 0.026	0.626 ± 0.003

Table 10: Univariate long-term series forecasting results on six datasets with input length $I = 96$ and prediction length $O \in \{96, 192, 336, 720\}$. A lower MSE indicates better performance. All experiments are repeated 5 times.

Methods	FiLM		FEDformer		Autoformer		S4		Informer		LogTrans		Reformer		
	Metric	MSE	MAE	MSE	MAE	MSE	MAE	MSE	MAE	MSE	MAE	MSE	MAE	MSE	MAE
ETTm2	96	0.065	0.189	0.063	0.189	0.065	0.189	0.153	0.318	0.088	0.225	0.075	0.208	0.076	0.214
	192	0.094	0.233	0.102	0.245	0.118	0.256	0.183	0.350	0.132	0.283	0.129	0.275	0.132	0.290
	336	0.124	0.274	0.130	0.279	0.154	0.305	0.204	0.367	0.180	0.336	0.154	0.302	0.160	0.312
	720	0.173	0.323	0.178	0.325	0.182	0.335	0.482	0.567	0.300	0.435	0.160	0.321	0.168	0.335
Electricity	96	0.154	0.247	0.253	0.370	0.341	0.438	0.351	0.452	0.484	0.538	0.288	0.393	0.274	0.379
	192	0.166	0.258	0.282	0.386	0.345	0.428	0.373	0.455	0.557	0.558	0.432	0.483	0.304	0.402
	336	0.188	0.283	0.346	0.431	0.406	0.470	0.408	0.477	0.636	0.613	0.430	0.483	0.370	0.448
	720	0.249	0.341	0.422	0.484	0.565	0.581	0.472	0.517	0.819	0.682	0.491	0.531	0.460	0.511
Exchange	96	0.110	0.259	0.131	0.284	0.241	0.387	0.344	0.482	0.591	0.615	0.237	0.377	0.298	0.444
	192	0.207	0.352	0.277	0.420	0.300	0.369	0.362	0.494	1.183	0.912	0.738	0.619	0.777	0.719
	336	0.327	0.461	0.426	0.511	0.509	0.524	0.499	0.594	1.367	0.984	2.018	1.070	1.832	1.128
	720	0.811	0.708	1.162	0.832	1.260	0.867	0.552	0.614	1.872	1.072	2.405	1.175	1.203	0.956
Traffic	96	0.144	0.215	0.170	0.263	0.246	0.346	0.194	0.290	0.257	0.353	0.226	0.317	0.313	0.383
	192	0.120	0.199	0.173	0.265	0.266	0.370	0.172	0.272	0.299	0.376	0.314	0.408	0.386	0.453
	336	0.128	0.212	0.178	0.266	0.263	0.371	0.178	0.278	0.312	0.387	0.387	0.453	0.423	0.468
	720	0.153	0.252	0.187	0.286	0.269	0.372	0.263	0.386	0.366	0.436	0.491	0.437	0.378	0.433
Weather	96	0.0012	0.026	0.0035	0.046	0.011	0.081	0.0061	0.065	0.0038	0.044	0.0046	0.052	0.012	0.087
	192	0.0014	0.029	0.0054	0.059	0.0075	0.067	0.0067	0.067	0.0023	0.040	0.0056	0.060	0.0098	0.079
	336	0.0015	0.030	0.0041	0.050	0.0063	0.062	0.0025	0.0381	0.0041	0.049	0.0060	0.054	0.0050	0.059
	720	0.0022	0.037	0.015	0.091	0.0085	0.070	0.0074	0.0736	0.0031	0.042	0.0071	0.063	0.0041	0.049
LLI	24	0.629	0.538	0.693	0.629	0.948	0.732	0.866	0.584	5.282	2.050	3.607	1.662	3.838	1.720
	36	0.444	0.481	0.554	0.604	0.634	0.650	0.622	0.532	4.554	1.916	2.407	1.363	2.934	1.520
	48	0.557	0.584	0.699	0.696	0.791	0.752	0.813	0.679	4.273	1.846	3.106	1.575	3.754	1.749
	60	0.641	0.644	0.828	0.770	0.874	0.797	0.931	0.747	5.214	2.057	3.698	1.733	4.162	1.847

C.5 ETT Full Benchmark

We present the full-benchmark on the four ETT datasets Zhou et al. (2021) in Table 11 (multivariate forecasting) and Table 12 (univariate forecasting). The ETTh1 and ETTh2 are recorded hourly while ETTm1 and ETTm2 are recorded every 15 minutes. The time series in ETTh1 and ETTm1 follow the same pattern, and the only difference is the sampling rate, similarly for ETTh2 and ETTm2. On average, our FiLM yields a **14.0%** relative MSE reduction for multivariate forecasting, and a **16.8%** reduction for univariate forecasting over the SOTA results from FEDformer.

D Parameter Sensitivity

Influence of legendre functon number N and frequency model number M The experiment results on three different dataset (ETTm1, Electricity, and Exchange) in Figure 7 shows the optimal choice of Legendre Polynomial number (N) when we aim to minimize the reconstruction error (in MSE) for the historical data. The MSE error decreases sharply at first and saturates at an optimal point, where N is in proportion to the input length. For 192, 336, and 720 input sequence, $N \approx 40$, 60, and 100 gives the minimal MSE respectively.

Figure 8 shows the MSE error of time series forecasting on Electricity dataset, with different Legendre Polynomial number (N), mode number and input length. We observe that, when enlarging N, the model performance increases at first and saturates at a point. For example, in Figure 8 Left (input length=192), the best performance is reached when N is larger than 64. While in Figure 8 Right (input length=720), the best performance is reached when N is larger than 128. Another influential parameter is the modes number. From Figure 8 we observe that a small mode number module works as a denoising filter.

Table 11: Multivariate long sequence time-series forecasting results on ETT full benchmark. The best results are highlighted in bold.

Methods	FiLM		FEDformer		Autoformer		S4		Informer		LogTrans		Reformer		
Metric	MSE	MAE	MSE	MAE	MSE	MAE	MSE	MAE	MSE	MAE	MSE	MAE	MSE	MAE	
<i>ETT_{h1}</i>	96	0.371	0.394	0.376	0.419	0.449	0.459	0.949	0.777	0.865	0.713	0.878	0.740	0.837	0.728
	192	0.414	0.423	0.420	0.448	0.500	0.482	0.882	0.745	1.008	0.792	1.037	0.824	0.923	0.766
	336	0.442	0.445	0.459	0.465	0.521	0.496	0.965	0.75	1.107	0.809	1.238	0.932	1.097	0.835
	720	0.465	0.472	0.506	0.507	0.514	0.512	1.074	0.814	1.181	0.865	1.135	0.852	1.257	0.889
<i>ETT_{h2}</i>	96	0.284	0.348	0.346	0.388	0.358	0.397	1.551	0.968	3.755	1.525	2.116	1.197	2.626	1.317
	192	0.357	0.400	0.429	0.439	0.456	0.452	2.336	1.229	5.602	1.931	4.315	1.635	11.12	2.979
	336	0.377	0.417	0.482	0.480	0.482	0.486	2.801	1.259	4.721	1.835	1.124	1.604	9.323	2.769
	720	0.439	0.456	0.463	0.474	0.515	0.511	2.973	1.333	3.647	1.625	3.188	1.540	3.874	1.697
<i>ETT_{m1}</i>	96	0.302	0.345	0.378	0.418	0.505	0.475	0.640	0.584	0.672	0.571	0.600	0.546	0.538	0.528
	192	0.338	0.368	0.426	0.441	0.553	0.496	0.570	0.555	0.795	0.669	0.837	0.700	0.658	0.592
	336	0.373	0.388	0.445	0.459	0.621	0.537	0.795	0.691	1.212	0.871	1.124	0.832	0.898	0.721
	720	0.420	0.420	0.543	0.490	0.671	0.561	0.738	0.655	1.166	0.823	1.153	0.820	1.102	0.841
<i>ETT_{m2}</i>	96	0.165	0.256	0.203	0.287	0.255	0.339	0.705	0.690	0.365	0.453	0.768	0.642	0.658	0.619
	192	0.240	0.313	0.269	0.328	0.281	0.340	0.924	0.692	0.533	0.563	0.989	0.757	1.078	0.827
	336	0.286	0.345	0.325	0.366	0.339	0.372	1.364	0.877	1.363	0.887	1.334	0.872	1.549	0.972
	720	0.393	0.422	0.421	0.415	0.422	0.419	2.074	1.074	3.379	1.338	3.048	1.328	2.631	1.242

Table 12: Univariate long sequence time-series forecasting results on ETT full benchmark. The best results are highlighted in bold.

Methods	FiLM		FEDformer		Autoformer		S4		Informer		LogTrans		Reformer		
Metric	MSE	MAE	MSE	MAE	MSE	MAE	MSE	MAE	MSE	MAE	MSE	MAE	MSE	MAE	
<i>ETT_{h1}</i>	96	0.055	0.178	0.079	0.215	0.071	0.206	0.316	0.490	0.193	0.377	0.283	0.468	0.532	0.569
	192	0.072	0.207	0.104	0.245	0.114	0.262	0.345	0.516	0.217	0.395	0.234	0.409	0.568	0.575
	336	0.083	0.229	0.119	0.270	0.107	0.258	0.825	0.846	0.202	0.381	0.386	0.546	0.635	0.589
	720	0.090	0.240	0.127	0.280	0.126	0.283	0.190	0.355	0.183	0.355	0.475	0.628	0.762	0.666
<i>ETT_{h2}</i>	96	0.127	0.272	0.128	0.271	0.153	0.306	0.381	0.501	0.213	0.373	0.217	0.379	1.411	0.838
	192	0.182	0.335	0.185	0.330	0.204	0.351	0.332	0.458	0.227	0.387	0.281	0.429	5.658	1.671
	336	0.204	0.367	0.231	0.378	0.246	0.389	0.655	0.670	0.242	0.401	0.293	0.437	4.777	1.582
	720	0.241	0.396	0.278	0.420	0.268	0.409	0.630	0.662	0.291	0.439	0.218	0.387	2.042	1.039
<i>ETT_{m1}</i>	96	0.029	0.127	0.033	0.140	0.056	0.183	0.651	0.733	0.109	0.277	0.049	0.171	0.296	0.355
	192	0.041	0.153	0.058	0.186	0.081	0.216	0.190	0.372	0.151	0.310	0.157	0.317	0.429	0.474
	336	0.053	0.175	0.071	0.209	0.076	0.218	0.428	0.581	0.427	0.591	0.289	0.459	0.585	0.583
	720	0.071	0.205	0.102	0.250	0.110	0.267	0.254	0.433	0.438	0.586	0.430	0.579	0.782	0.730
<i>ETT_{m2}</i>	96	0.065	0.189	0.063	0.189	0.065	0.189	0.153	0.318	0.088	0.225	0.075	0.208	0.076	0.214
	192	0.094	0.233	0.102	0.245	0.118	0.256	0.183	0.350	0.132	0.283	0.129	0.275	0.132	0.290
	336	0.124	0.274	0.130	0.279	0.154	0.305	0.204	0.367	0.180	0.336	0.154	0.302	0.160	0.312
	720	0.173	0.323	0.178	0.325	0.182	0.335	0.482	0.567	0.300	0.435	0.160	0.321	0.168	0.335

E Noise Injection Experiment

Our model’s robustness in long-term forecasting tasks can be demonstrated using a series of noise injection experiments as shown in Table 13. As we can see, adding a gaussian noise in the training/test stage have limited effect on our model’s performance, the deterioration is less than 1.5% in the worst case. The model’s robustness is consistent across various of forecasting length. Note that adding the noise in testing stage other than the training stage will even improve our performance by 0.4%, which further supports our claim of robustness .

F Distribution Analysis of Forecasting Output

F.1 Kolmogorov-Smirnov Test

We adopt Kolmogorov-Smirnov (KS) test to check whether the two data samples come from the same distribution. KS test is a nonparametric test of the equality of continuous or discontinuous, two-dimensional probability distributions. In essence, the test answers the question “what is the probability that these two sets of samples were drawn from the same (but unknown) probability distribution”. It quantifies a distance between the empirical distribution function of two samples.

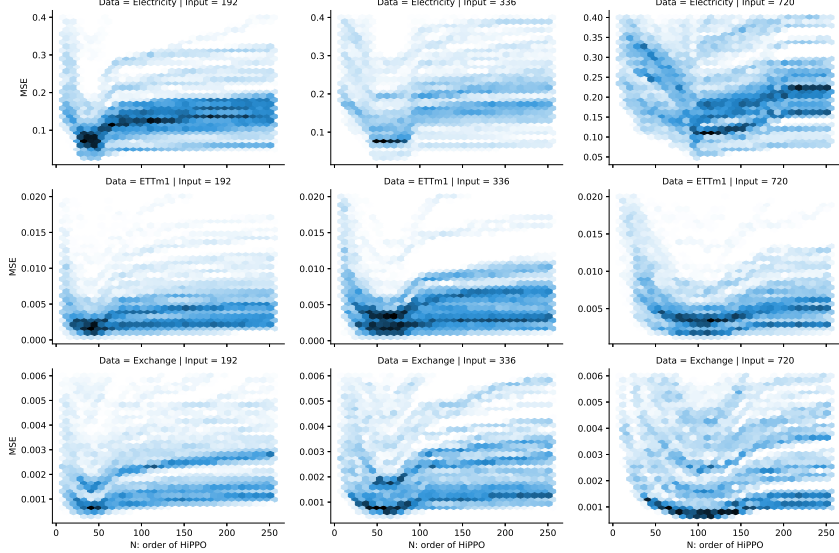


Figure 7: The reconstruction error (MSE) vs order of Legendre Function (N) on three datasets with three different input length.

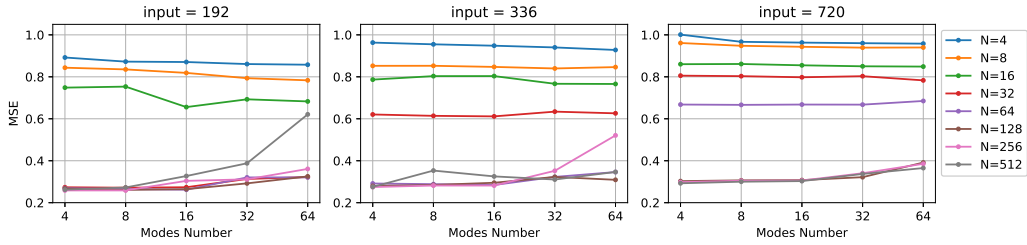


Figure 8: The MSE error of univariate time series forecasting task on Electricity dataset with different Legendre Polynomial number (N), mode number and input length. Left: input length is 192. Mid input length is 336. Right: input length is 720.

The Kolmogorov-Smirnov statistic is

$$D_{n,m} = \sup_x |F_{1,n}(x) - F_{2,m}(x)|$$

where $F_{1,n}$ and $F_{2,m}$ are the empirical distribution functions of the first and the second sample respectively, and \sup is the supremum function. For large samples, the null hypothesis is rejected at level α if

$$D_{n,m} > \sqrt{-\frac{1}{2} \ln \left(\frac{\alpha}{2} \right)} \cdot \sqrt{\frac{n+m}{n \cdot m}},$$

where n and m are the sizes of the first and second samples respectively.

F.2 Distribution Analysis

In this section, we evaluate the distribution similarity between the input sequence and forecasting output of different transformer models quantitatively. In Table 14, we applied the Kolmogorov-Smirnov test to check if the forecasting results of different models made on ETTm1 and ETTm2 are consistent with the input sequences. In particular, we test if the input sequence of fixed 96-time steps come from the same distribution as the predicted sequence, with the null hypothesis that both sequences come from the same distribution. On both datasets, by setting the standard P-value as 0.01, various existing Transformer baseline models have much fewer values than 0.01 except Autoformer, which indicates their forecasting output has a higher probability of being sampled from the different distributions than the input sequence. In contrast, FiLM, Autoformer, and Fedformer have much larger

Table 13: Noise injection studies. A $0.3\mathcal{N}(0, 1)$ gaussian noise is introduced into our training/testing. We conduct 4 sets of experiments with w/wo noise in training and w/wo noise in testing phase. The experiments are performed on ETTm1 and Electricity with different output length. The metric of variants is presented in relative value ('+' indicates degraded performance, '-' indicates improved performance).

Training	without Noise				with Noise				
Testing	WO Noise		W Noise		WO Noise		W Noise		
Metric	MSE	MAE	MSE	MAE	MSE	MAE	MSE	MAE	
<i>ETTh1</i>	96	0.371	0.394	-1.6%	-2.0%	-0.0%	-0.0%	-1.6%	-2.0%
	192	0.414	0.423	-0.5%	-1.4%	+0.5%	-0.0%	-0.5%	-1.4%
	336	0.442	0.445	-1.8%	-0.9%	-0.9%	+1.3%	-3.2%	-1.6%
	720	0.465	0.472	+0.2%	-0.2%	+0.9%	+0.9%	-0.6%	-0.4%

Table 14: P-values of Kolmogorov-Smirnov test of different transformer models for long-term forecasting output on ETTm1 and ETTm2 dataset. Larger value indicates the hypothesis (the input sequence and forecasting output come from the same distribution) is less likely to be rejected. The largest results are highlighted.

Methods	Transformer	Informer	Autoformer	FEDformer	FiLM	True	
ETTm1	96	0.0090	0.0055	0.020	0.048	0.016	0.023
	192	0.0052	0.0029	0.015	0.028	0.0123	0.013
	336	0.0022	0.0019	0.012	0.015	0.0046	0.010
	720	0.0023	0.0016	0.008	0.014	0.0024	0.004
ETTm2	96	0.0012	0.0008	0.079	0.071	0.022	0.087
	192	0.0011	0.0006	0.047	0.045	0.020	0.060
	336	0.0005	0.00009	0.027	0.028	0.012	0.042
	720	0.0008	0.0002	0.023	0.021	0.0081	0.023

P-values than others, mainly contributing to their seasonal-trend decomposition mechanism. The proposed FiLM has a much larger P-value than the transformer/informer model. And it's null hypothesis can not be rejected with a P-value larger than 0.01 in all cases of the two datasets. It implies that the output sequence generated by FiLM shares a more similar distribution as the input sequence and thus justifies our design motivation of FiLM as discussed in Section 1. Though FiLM gets a smaller P-value than Fedformer, it is close to the actual output, making a good balance between recovering and forecasting.

G Learnable Parameter Size

Table 15: Parameter size for baseline models and FiLM with different low-rank approximations: the models are trained and tested for ETT dataset. the subscript number is k value for LRA

Methods	Transformer	Autoformer	FEDformer	FiLM	FiLM ₁₆	FiLM ₄	FiLM ₁
Parameter(M)	0.0069	0.0069	0.0098	1.50	0.0293	0.0062	0.00149

Compared to Transformer-based baseline models, FiLM can enjoys a lightweight property with **80%** learnable parameter reductions as shown in Table 15. It has the potential to be used in mobile devices, or, in some situations, require a lightweight model.

H Training Time and Memory Usage

As shown in Figure 9, FiLM has a good linear time and memory usage with the prolonging input length. Note that the absolute running time is and memory usage is relatively high due to the heavy projection step and the resulting large intermediate tensor. We will elaborate on the efficient implementation of FiLM in the future.

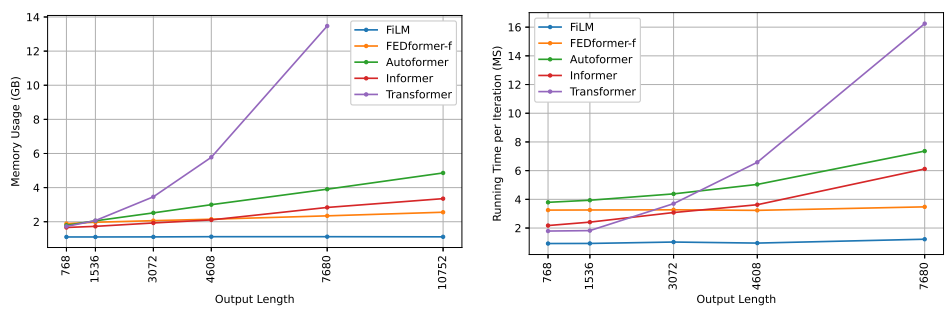


Figure 9: (Left) the memory usage of FiLM and baseline models. (Right) training speed of FiLM and baseline models.